Thermal Aging of Heterophasic Propylene−Ethylene Copolymers: Morphological Aspects Based on ESR, FTIR, and DSC

Krzysztof Kruczala,† Biji Varghese, Jayesh G. Bokria, and Shulamith Schlick*

Department of Chemistry, University of Detroit Mercy, Detroit, Michigan 48219

Received September 30, 2002; Revised Manuscript Received January 10, 2003

ABSTRACT: Electron spin resonance (ESR) spectra of nitroxide radicals formed in thermally treated heterophasic propylene−ethylene copolymers (HPEC) containing bis(2,2,6,6-tetramethyl-4-piperidinyl) sebacate (Tinuvin 770) as a hindered amine stabilizer (HAS) were studied in the temperature range 100−433 K; the nitroxides are derived from the HAS and are termed *HAS−NO*. The results were compared with ESR spectra of the same radicals obtained first by oxidation of Tinuvin 770 and then doped in HPEC and related homopolymers polyethylene (PE) and polypropylene (PP); these nitroxides are termed *spin probes*. ESR spectra indicated that HAS−NO and the spin probes in HPEC and homopolymers reside in a range of amorphous sites differing in their dynamical properties. Evidence for the various sites was obtained from the ESR line widths, the temperature variation of the extreme separation in the ESR spectra, and the effect of stress on the ratio of the *fast* and *slow* components in the spectra of HAS−NO in thermally treated HPEC. The relative population of sites was explained by assuming that the crystalline domains exert a restraining effect on chains located in vicinal amorphous domains; in PE the restraining effect was more pronounced in the polymer with the higher crystallinity (HDPE vs LDPE). Additional support for this assumption was provided by Fourier transform infrared (FTIR) spectra of HPEC and related polymers and by differential scanning calorimetry (DSC). The dynamically restrained chains evidenced by the spin probes are thought to be located in a *rigid amorphous phase*, which was described in the literature. In HPEC the fast spectral component represents unrestrained ethylene−propylene rubber (EPR) chains, and the slow spectral component represents amorphous PP and EPR chains in the rigid amorphous phase. This study has demonstrated the exceptional sensitivity of ESR spectra from nitroxide radicals to polymer morphology and degree of crystallinity.

Introduction

Heterophasic propylene−ethylene copolymers (HPEC), known commercially as impact polypropylene copolymers (IPC), are an important class of polymers, due to their attractive mechanical properties and low cost.[1] The polymers consist of crystalline polypropylene (PP) modified by an elastomeric component, typically ethylene−propylene rubber (EPR).[2] HPEC are prepared by polymerization of propylene (P) in the presence of catalysts, and sequential polymerization of a propylene−ethylene mixture with the same catalysts.[3] Resulting polymeric materials are heterophasic, but the specific morphology depends on the preparation method and monomer ratio.

In scanning electron microscopy (SEM) studies of HPEC, evidence for the presence of "two phases" has been reported:[4] the continuous PP phase and the dispersed EPR phase. The size of the dispersed elastomer particles was found to depend on the polymerization details; for HPEC prepared by sequential polymerization and containing 18 wt % EPR, for example, the particle size measured by SEM was $\leq 1\ \mu$m.[4] More recent papers have recognized the presence of *four* phases: crystalline PP, amorphous PP, crystalline EPR (predominantly polyethylene, PE), and amorphous EPR.[5−11] The composition of the phases has been studied by FTIR, DSC, wide-angle X-ray scattering (WAXS), and nuclear magnetic resonance (NMR); some studies were performed on fractions obtained by temperature-gradient extraction fractionation (TGEF), a method based on the higher dissolution temperature of crystalline domains, compared to amorphous domains. While some methods, for instance FTIR, are suitable for the detection of all phases, probe methods such as ^{129}Xe NMR report only on the amorphous phases.[4b,5] In some papers HPEC and PP/EPR blends are termed thermoplastic polyolefins (TPO).[3,12,13]

The morphology of HPEC is of considerable interest because processing at high temperatures can lead to morphological changes. An understanding of the morphology and of the temperature dependence of the domain size has enormous practical importance. For samples prepared by injection molding of PP/EPR blends, depth-profiling studies have revealed a skin consisting of several layers ("stratification"), whose composition is different compared to the bulk phase;[12,13] the effect was explained by postprocessing temperature variations in the sample upon cooling. Similar effects have been detected earlier in PP samples and assigned to flow, shear, and temperature variations during and following processing.[14]

As the related homopolymers PP and PE, HPEC are vulnerable to degradation upon exposure to radiation and/or heat in the presence of oxygen and can be used commercially only if stabilized by antioxidants or radical scavengers. For this reason, our initial objective was to study spatial effects in the degradation of HPEC containing a hindered amine stabilizer (HAS), with methods developed and used in our study of degradation in UV-irradiated and heat-treated poly(acrylonitrile−butadiene−styrene) (ABS) containing HAS:[15] The major method of study was 1D and 2D electron spin resonance imaging (ESRI) based on the formation of nitroxide radicals from the HAS during aging. Deductions from the ESRI experiments were supported by the spin probe

† On leave from the Faculty of Chemistry, Jagiellonian University, Cracow, Poland.

* Corresponding author. E-mail schlicks@udmercy.edu.

10.1021/ma025700y CCC: $25.00
Published on Web 02/22/2003

Table 1. Polymers Studied

polymer	source	molecular mass	other properties
polypropylene (iPP)	Aldrich	250 000 (M_w) 67 000 (M_n)	isotactic density = 0.900 g/mL
low-density polyethylene (LDPE)	SP[2]	50 000 (M_w)	pellets density = 0.92 g/mL
high-density polyethylene (HDPE)	SP[2]	125 000 (M_w)	pellets density = 0.95 g/mL
HPEC1	Dow	227 000 (M_w) 60 700 (M_n)	pellets
HPEC2	Dow	428 000 (M_w) 90 400 (M_n)	pellets

study of ABS and related polymers[16] and by attenuated total reflectance (ATR) FTIR spectra of microtomed layers (50 μm thick) of the polymer.[17]

Our expectation was that the clear connection between phase heterogeneity and degradation, which was key to the interpretation of the results in ABS, would also be applicable to the HPEC system. Initial experiments demonstrated, however, that HPEC is more complicated because of the presence of amorphous *and* crystalline domains. Numerous studies of polymer dynamics based on ESR spectra of nitroxide spin probe, including our previous work, have demonstrated that nitroxide spin probes reside only in amorphous phases. Our experiments on HPEC suggested, however, that stress leads to changes in the ESR spectra of probes. We explained this result by assuming that stress leads to additional ordering and that the crystalline phases, although not directly represented in the ESR spectra, have a subtle but important effect on the spectra of probes residing in the amorphous phases. Therefore, deductions made on the degradation processes from the spatial variation of intensities and line shapes of the fast (F) and slow (S) nitroxide components must also take into account morphological changes. A study on the morphological aspects during aging of HPEC, and comparison with related polymers, became essential and is presented in this paper. The methods used are spin probe ESR, study of HAS-derived nitroxides (HAS−NO) formed by heating HPEC samples containing HAS, FTIR, and DSC. The following paper describes 1D and 2D ESRI and FTIR studies of thermal aging in HPEC.[18]

Experimental Section

Materials. Isotactic polypropylene (iPP) was obtained from Aldrich. Low-density and high-density polyethylene, LDPE and HDPE, respectively, were from Scientific Polymer Products (SP[2]). Two HPEC samples differing in their ethylene (E) content were from The Dow Chemical Co.: HPEC1 (IPC, C 708, M_n = 60 700, M_w = 227 000), and HPEC2 (IPC, C104-01, M_n = 90 400, M_w = 428 000). The amount of E in the HPEC samples was measured by preparing a calibration curve based on IR spectra of iPP and LDPE mixtures with known compositions, as described below. The results showed that the E content is 25 wt % in HPEC1 and 10 wt % in HPEC2, within ±2%. Table 1 summarizes the polymer sources and some properties.

The nitroxide spin probe was prepared by oxidation of bis-(2,2,6,6-tetramethyl-4-piperidinyl) sebacate (Tinuvin 770 from Ciba Specialty Chemicals, Chart 1) with *m*-chloroperoxybenzoic acid (*m*CPBA) and was a mixture of mono- and biradicals.[19] Although the nitroxide radicals studied have the same chemical structure, we will make a distinction between radicals formed in situ by thermal aging in HPEC plaques containing HAS, for which the notation is *HAS−NO*, and those doped in the polymers, for which the notation is *spin probes*.

Sample Preparation. HPEC samples containing 1 wt % Tinuvin 770, as plaques prepared by injection molding,[15] were

Chart 1. Hindered Amine Stabilizer (HAS) Tinuvin 770

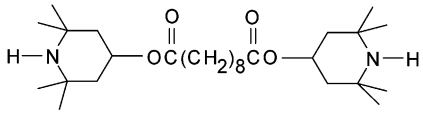

aged in a convection oven at 393 and 433 K. For the ESR experiments, cylindrical samples ≈7 mm in diameter were cut from the plaques with a hollow cylindrical tool at selected time intervals; the cutouts were trimmed to ≈4 mm and placed in the ESR resonator with the symmetry axis along the long (vertical) axis of the resonator. In the ESR imaging experiments this was also the direction of the magnetic field gradient. The ESR spectra of HAS−NO radicals were measured in the temperature range 100−433 K as a function of treatment time. Some ESR spectra of layers obtained by microtoming the cylinders were also measured. Slices of thickness 50 μm were obtained at room temperature, using a Spencer-820 rotatory microtome equipped with a stainless steel knife.

Polymers doped with spin probes are usually prepared by the dissolution method, which involves solubilization of the polymer and probe in the solvent, followed by solvent evaporation. This was the method used in the case of ABS polymers doped with spin probes.[16] LDPE is soluble in hexanes at ≈350 K. Dissolution of the HPEC, PP, and HDPE can be achieved in xylene at ≈400 K, but the solubilization process is slow and sometimes incomplete. For this reason, in this study the polymers were doped with the spin probe by the melting method: weighed amounts of the probe and polymer were mixed slightly above the melting point of the polymer.[20−23] Typical temperatures for mixing polymers and spin probe were ≈450 K for HPEC and PP and ≈400 K for HDPE and LDPE. The mixtures were held at the high temperature for ≈4 min or less in most cases.

ESR Measurements. Spectra were recorded with Bruker X-band EMX spectrometers operating at 9.7 GHz with 100 kHz magnetic field modulation and equipped with the Acquisit 32 Bit WINEPR data system version 3.01 for acquisition and manipulation and the ER 4111 VT variable temperature units. The microwave frequency was measured with a Hewlett-Packard 5350B microwave frequency counter. Most spectra were collected with the following parameters: sweep width 120 G, microwave power 2 mW, time constant 40.96 ms, conversion time 81.92 ms, 4−10 scans, and 1024−2048 points. In the case of iPP the signals from the spin probe were very broad, especially at the lower temperatures, and the sweep was increased up to 250 G. The modulation amplitude was varied in the range 0.5−1.2 G, depending on the line width. The temperature was controlled within ±1 K. All samples were allowed to equilibrate for at least 10 min after reaching the desired temperature. Additional experimental details have been described.[15,16]

FTIR Measurements. Spectra of films from HPEC1, HPEC2, PP, HDPE, LDPE, and PP/LDPE mixtures were acquired in the transmission mode using the Perkin-Elmer Spectrum 2000 FTIR spectrometer equipped with a mid-IR (MIR) globar source and a triglycine sulfate (TGS) detector. To obtain the films, polymer pellets placed on Al foil were

compression-molded between two preheated flat molds in a Carver press for 30 s at ≈475 K and a pressure of 1600 atm. Transmission spectra from the films were acquired in the range 4000−400 cm^{-1}, with a resolution of 4 cm^{-1}; eight scans were collected and corrected for open-beam background. During acquisition, the film was held in place with a magnetic film holder.

The amount of ethylene (E) in the HPEC samples was deduced from the ratio of absorbances at 1167 and 720 cm^{-1}, A_{1167}/A_{720}. A calibration curve was constructed by analyzing the IR spectra of iPP/LDPE mixtures with known E content. Mixtures containing 5, 10, 15, 20, 25, and 30 wt % LDPE were prepared and mixed in an aluminum pan above the melting points of the polymers. After cooling, the mixture was cut into small pieces and molded into a sheet; this process was repeated 3−4 times to ensure maximum possible homogeneity. From the final molded plate, 4−6 films were compression-molded using aluminum foil as a spacer between the molds. The average absorbance ratio A_{1167}/A_{720} in the films prepared from each mixture was plotted as a function of wt % E. The % E corresponding to the measured A_{1167}/A_{720} ratio in HPEC1 and HPEC2 was then read from the calibration curve.

DSC Measurements. Thermal transitions were measured with a DuPont 9900/TA Instruments calorimeter calibrated with mercury (mp 234.28 K) and indium (mp 429.71 K) standards.

Simulation of ESR Spectra. The rotational diffusion of the probes was simulated on the basis of an axially symmetric rotational diffusion model. The dynamics of the probe is defined by $R_{\|}$ and $R_{\perp}$, the components of the rotational diffusion tensor parallel and perpendicular, respectively, to the symmetry axis of the rotational diffusion tensor and by the diffusion tilt angle, ϑ, between the symmetry axis of the rotational diffusion tensor and the z axis of the nitroxide axis system; z is the symmetry axis of the nitrogen $2p_z$ atomic orbital, and the N−O bond is along x.

The ESR spectra were calculated using the simulation method based on the stochastic Liouville equation and fitted to the experimental spectra using the iterative nonlinear least-squares fitting program (NLSL) based on a modified Levenberg−Marquart minimization algorithm.[24] The peak-to-peak line widths of the first-derivative signals, $H_{\|}$ and $H_{\perp}$, were variable parameters, in addition to $R_{\|}$ and $R_{\perp}$. In all simulations we chose $\vartheta = 90°$.[15a] The line shapes were a mixture of Gaussian and Lorentzian functions.

The first step in the simulation procedure was the choice of **A** and **g** tensors. The principal values of the tensors for the spin probe cannot be determined directly and accurately from the low-temperature (120 K) ESR spectra because of the very broad lines; some of the broadening may be due to the presence of two NO groups in one probe molecule at distances larger than that giving rise to the five-line biradical spectrum but smaller than the fully extended conformation. By comparison with the principal values used for simulation of HAS−NO spectra in ABS,[15a] the following tensor components were selected: $g_{xx} = 2.0088$, $g_{yy} = 2.0061$, $g_{zz} = 2.0027$ and $A_{xx} = 6.3$ G, $A_{yy} = 5.8$ G, and $A_{zz} = 33.6$ G. On the basis of our previous experience and the current literature on simulating ESR spectra of relatively large probes,[16b,24] the strong jump diffusion model was adopted for the simulation of the ESR spectra of the spin probe in iPP. In this model the spin probe has a fixed orientation for time τ_R and then jumps instantaneously to a new orientation. For the strong diffusion model the rotational correlation time is $\tau_R = 7/(6\sqrt{R_{\|}R_{\perp}})$.[16b,24]

Results

ESR Spectra of HAS−NO in HPEC1 and HPEC2. In Figure 1A we present selected ESR spectra in the temperature range 120−360 K for HAS−NO in HPEC1 thermally treated at 393 K for 107 days. The rigid limit spectrum at 120 K changed as the temperature increased, and at 300 K the dynamically fast (F) component emerged. The line shapes at 360 K are typical for the rotation of the probe along the long axis, x, of HAS−NO ($\vartheta = 90°$).[15a] Similar spectra were observed for HPEC2; the spectrum at 300 K of HAS−NO in HPEC2 that was similarly treated is shown in Figure 1B. Inspection of the spectra at 300 K indicates that the relative intensity of the F component is lower in HPEC2 compared to HPEC1.

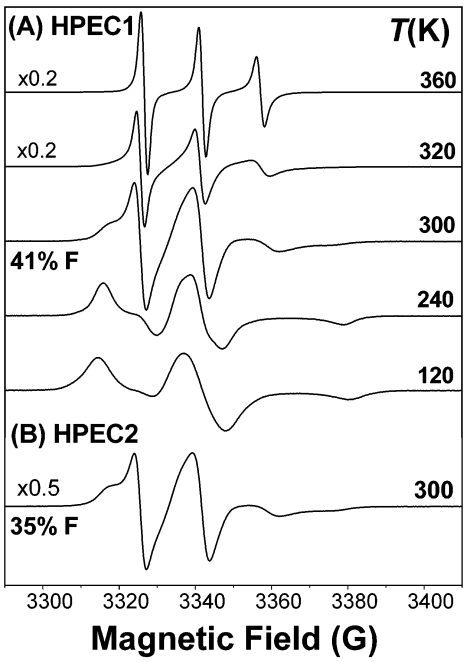

Figure 1. ESR spectra of HAS−NO in HPEC1 and HPEC2 thermally treated at 393 K for 107 days. (A) Selected spectra in HPEC1 at the indicated temperatures. (B) Spectrum at 300 K in HPEC2. The % F at 300 K is indicated in (A) and (B).

Typical melting points for the HPEC components are 395 K for crystalline PE and ≈441 K for crystalline PP (see below DSC data). A probe molecule located in crystalline domains is expected to be represented, below the polymer melting point, by a dynamically slow (S) spectral component. In the spectra shown in Figure 1, however, the slow component is not visible above 320 K, indicating that HAS−NO is *not* located in crystalline domains. Therefore, the nitroxide radicals reflect the dynamics in the amorphous domains. It is reasonable to extend this conclusion to the location of the spin probe in the homopolymers and HPEC samples, to be described in the next section.

The relative intensities of the two spectral components in the HPEC samples were deduced by deconvolution: The ESR spectrum of HPEC2 at 300 K was subtracted from that of HPEC1 at the same temperature, and the result was the F component. In the second step the F component was subtracted from a composite spectrum in order to isolate the S component. The two components were then superimposed in varying relative intensities in order to reproduce the experimental spectra. For polymers treated at 393 K for 107 days, % F = 41 in HPEC1 and 35 in HPEC2 in spectra measured at 300 K, within ±2%. In ABS polymers the F component was assigned to radicals located in the elastomer (polybutadiene) phase,[15,16] and % F correlated with the butadiene (B) content in three ABS polymers with B contents of 10, 25, and 45 wt %. Initially, a similar assignment of the F component, to the EPR component in HPEC, was considered. The ratio of % F values in the two HPEC samples is 1.2, and the corresponding %

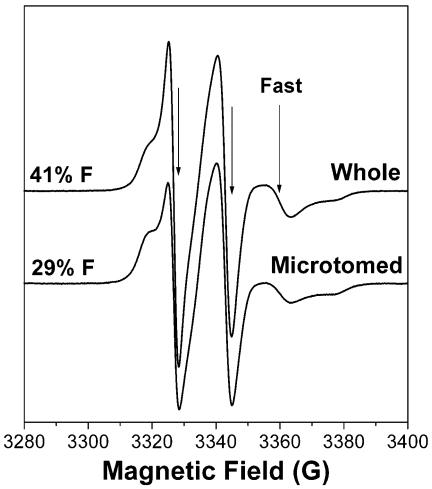

Figure 2. ESR spectra of HAS−NO at 300 K in whole and in microtomed HPEC1 after thermal treatment at 393 K for 107 days. The % F is indicated.

E ratio is ≈2.5; this ratio is therefore not strictly correlated with the EPR content. Below we will elaborate on the significance of % F in the HPEC polymers by considering additional data.

Effect of Stress on % F in HPEC. While performing the ESR and ESRI experiments, we observed that cylindrical samples cut with a cutting tool of diameter 5 mm contained a lower % F in their ESR spectra at 300 K, compared to samples cut with a tool of larger diameter, 7 mm, and trimmed to fit the 5 mm in diameter ESR sample tube. A series of controlled experiments were then performed in order to quantify the effect, and the results are shown in Figure 2. The upper spectrum was measured at 300 K for HAS−NO in HPEC1 aged at 393 K for 107 days; the cylindrical sample was obtained with a cutting tool of diameter 7 mm and then trimmed by a sharp blade to fit the ESR tube; in this sample % F = 41 ± 2. The same sample was subsequently microtomed into 50 μm slices, followed by the transfer of all slices to the ESR sample tube; in the ESR spectrum of the slices (bottom spectrum in Figure 2) % F = 29 ± 2. The lowering of the relative intensity of the F nitroxide component in the amorphous phase is assigned to the increased degree of order as a result of microtoming.[13] The decrease of % F was not the only result of microtoming: The extreme separation measured immediately after microtoming was unchanged but increased over a period of several days by ≈1 G at 300 K; the increase was detected in all ESR spectra measured in the temperature range 100−300 K. The lowering of % F and increasing extreme separation are assigned to increased ordering and further crystallization upon microtoming. To the best of our knowledge, the restraining effect of chains in the crystalline domains on ESR spectra of nitroxide radicals located in amorphous domains is reported here quantitatively for the first time. These ESR spectra have great sensitivity because the effect is observed mainly on the amorphous component with narrow lines (the fast component) and leads to large differences in the *height* of the corresponding signals.

Additional support for the restraining effect of the crystalline domains came from the observation of broader lines for the F component after long (>10 days) thermal treatment at 433 K. As significant degradation was detected under these conditions,[18] further crystallization

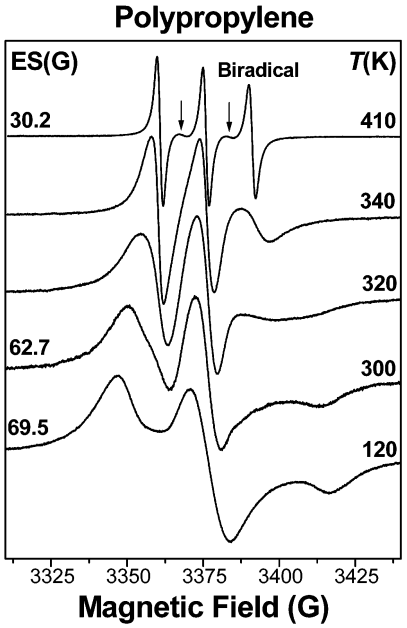

Figure 3. ESR spectra of the spin probe in iPP at the indicated temperatures. The extreme separation, ES(G), is given for some spectra. Arrows point to the signal from the biradicals, 2NO−HAS, in the spectrum measured at 410 K.

is expected because chain scission results in shorter chains that can more easily rearrange into crystalline domains. This effect is well established for PP and known as chemicrystallization.[25,26] In the case of HPEC, the higher degree of crystallinity further restrains the chains in amorphous domains, and the result is slower dynamics and broader lines in ESR spectra. The broader lines may also suggest that a higher degree of crystallinity leads to a *range* of amorphous domains that differ in their dynamical properties, as chains in amorphous domains closer to the crystalline domains are more motionally restrained; a gradient of dynamics in the amorphous phase is formed. This idea is supported by the ESR spectra of the spin probe in the homopolymers, which are presented below.

ESR Spectra of the Spin Probe in Homopolymers and HPEC. The ESR spectrum of the biradical 2NO−HAS (*two* NO groups derived from Tinuvin 770) was detected in HPEC samples that were thermally treated at 433 K. We note that the relative amounts of the bi- and monoradical derived from HAS and in the spin probe may be different. Spectra typical of two interacting ⟩NO groups (five-line spectrum) in a long molecule such as Tinuvin 770 can be expected only in fluid media and will not interfere with the interpretation of the ESR spectra from the monoradical measured at lower temperatures. In support of this assumption, we recall that the ESR spectrum of HAS−NO at 300 K in polybutadiene, which has a lower glass transition compared to polymers based on P and E units, was simulated by assuming a rotation about the long axis of the HAS,[15a] indicating a rigid probe conformation. Therefore, it is appropriate to compare the ESR spectra of HAS−NO (in the thermally treated samples) with spectra of the spin probe doped in HPEC and homopolymers.

In Figure 3 we present selected spectra of the spin probe in iPP in the range 120−410 K. The lines are broad, not only at the lower temperature (rigid limit) but also in the entire temperature range. At 360 K for

Table 2. Dynamical Parameters (rad/s) and Line Widths (G) Used for the Simulation of ESR Spectra for the Spin Probe in IPP[a]

	$\Delta H_\perp$ (G)	$\Delta H_\parallel$ (G)	$R_\perp \times 10^{-5}$	$R_\parallel \times 10^{-8}$	τ_c (s/rad)
0 days	4	3.6	7.190	2.436	8.815E−08[b]
4 days	5.5	5.7	4.750	1.610	1.334E−07
7 days	5.8	7	4.043	1.370	1.568E−07
9 days	6	6.8	4.043	1.370	1.568E−07
20 days	5	5.5	3.603	1.221	1.759E−07

[a] In all simulations we have used $N = R_\parallel/R_\perp = 339$. [b] Read as 8.815×10^{-8}.

instance the three signals have line widths of 2.1, 2.7, and 5.2 G, respectively; these widths can be compared with line widths of 1.35, 1.35, and 1.79 G, respectively, measured for the spin probe 10-doxylnonadecane (10DND) in polybutadiene at 360 K. Above 400 K signals from the biradical, 2NO−HAS, appeared and are shown by arrows in Figure 3.

The variation of the ESR spectra of the spin probe in iPP as a function of time after sample preparation is shown in Figure 4A. The spectra at 300 K indicate the broadening of the lines over 20 days and the accompanying increase in the extreme separation from 57.2 to 62.7 G. The extreme separation at 120 K shows a small but measurable increase, from 69.2 G after 9 days to 69.5 G after 20 days. Simulated spectra are shown by dotted lines in Figure 4A; the spectra were calculated for identical magnetic parameters (**g** and ^{14}N hyperfine tensors) but different line widths and dynamic parameters. The parameters used to simulate the spectra are given in Table 2. The sensitivity of the calculated spectrum to the simulation parameters is shown in Figure 4B for the spectrum measured at 300 K, 7 days after sample preparation.

We assigned the exceptionally broad lines in iPP to a distribution of sites for the nitroxides, leading to a superposition of signals from multiple domains with a range of dynamical properties: probes located closer to the PP crystals are motionally constrained to a larger degree than probes located in more distant amorphous regions, away from the crystalline regions. The general picture of a *range* of amorphous phases, with a distribution of dynamics, is a result of the high crystallinity, ≈58%, calculated from the PP density.[27] We also note the absence of a fast component.

In Figure 5 we present selected ESR spectra of the spin probe in HDPE (Figure 5A) and LDPE (Figure 5B). The degree of crystallinity was 69% for HDPE vs 44% for LDPE, calculated from the corresponding densities.[27] This difference leads to important differences in the ESR spectra of the spin probe in the two polymers. First, at a given temperature, the extreme separation is higher in HDPE compared to LDPE: At 260 K, for example, the extreme separation is 64.2 G in HDPE and only 60.5 G in LDPE. Second, the spectra for LDPE at and above 290 K consist of broad lines that represent a superposition of probe sites, all near or in the motionally averaged regime; in HDPE, however, a slow component is also seen in the temperature range 300−320 K, which can be assigned to amorphous regions under the restraining effect of the crystalline domains. A range of dynamics in amorphous domains is clearly confirmed. Third, the more open structure in LDPE compared to HDPE is also reflected in the spectra at high temperatures: The biradical is seen in LDPE at 380 K, and the signal is stronger at 400 K (Figure 5B); in HDPE the biradical signals are less intense and appear only at 390 K (Figure 5A).

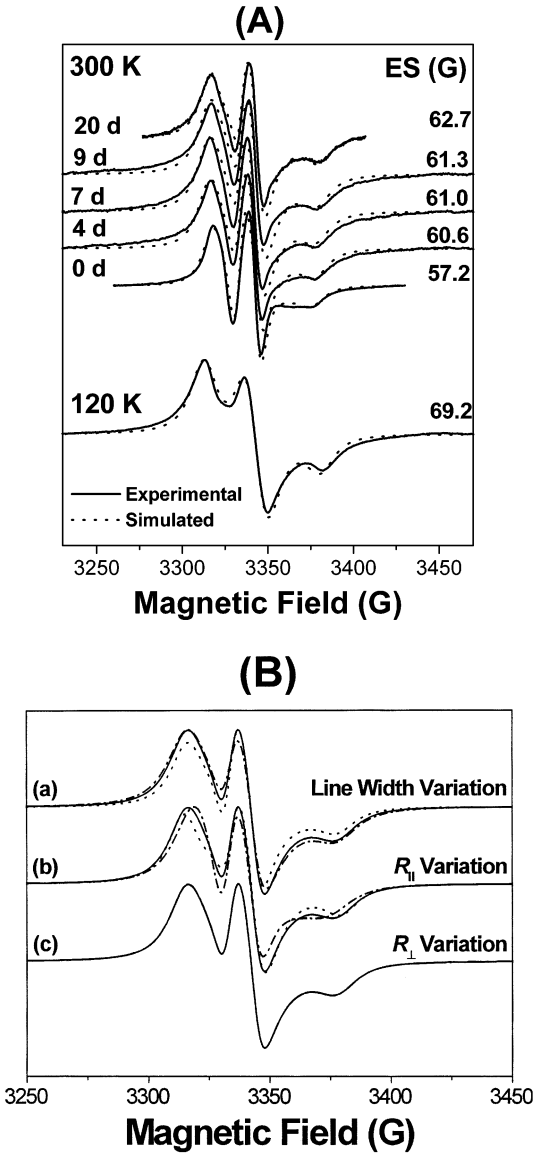

Figure 4. (A) ESR spectra of the spin probe in iPP at 300 and 120 K as a function of time after sample preparation. The extreme separation is shown on the right side of each spectrum. The corresponding simulated spectra are indicated by dotted lines. (B) Effect of parameter variation on the simulated spectra. The solid lines in (a), (b), and (c) are the simulated spectra of the spin probe in PP at 300 K after 7 days of sample preparation as shown in Figure 4 ($R_\perp = 4.0 \times 10^5$ rad/s, $R_\parallel = 1.3 \times 10^8$ rad/s, $\Delta H_\parallel = 5.8$ G, $\Delta H_\perp = 7.0$ G). (a) Effect of line width variation: $R_\perp = 4.0 \times 10^5$ rad/s, $R_\parallel = 1.3 \times 10^8$ rad/s, $\Delta H_\parallel = 4.8$ G, $\Delta H_\perp = 6.0$ G) (dotted line) and $R_\perp = 4.0 \times 10^5$ rad/s, $R_\parallel = 1.3 \times 10^8$ rad/s, $\Delta H_\parallel = 6.8$ G, $\Delta H_\perp = 8.0$ (dash dot). (b) Effect of $R_\parallel$ variation: $R_\perp = 4.0 \times 10^5$ rad/s, $R_\parallel = 0.65 \times 10^8$ rad/s, $\Delta H_\parallel = 5.8$ G, $\Delta H_\perp = 7.0$ G (dotted lines) and $R_\perp = 4.0 \times 10^5$ rad/s, $R_\parallel = 2.6 \times 10^8$ rad/s, $\Delta H_\parallel = 5.8$ G, $\Delta H_\perp = 7.0$ G (dash dot). (c) Effect of $R_\perp$ variation: $R_\perp = 0.8 \times 10^5$ rad/s, $R_\parallel = 1.3 \times 10^8$ rad/s, $\Delta H_\parallel = 5.8$ G, $\Delta H_\perp = 7.0$ G (dotted lines) and $R_\perp = 20.0 \times 10^5$ rad/s, $R_\parallel = 1.3 \times 10^8$ rad/s, $\Delta H_\parallel = 5.8$ G, $\Delta H_\perp = 7.0$ G (dash dot). The three traces in (c) are superimposed.

In Figure 6 we present selected ESR spectra of the spin probe in HPEC1 (Figure 6A) and HPEC2 (Figure 6B). The most important feature is the presence of two spectral components in the temperature range 300−320 K; % F = 36 in HPEC1 compared to 29 in HPEC2. The % F is slightly lower than that detected for the HAS−NO in HPEC (41 and 35%; see Figure 1) because of the

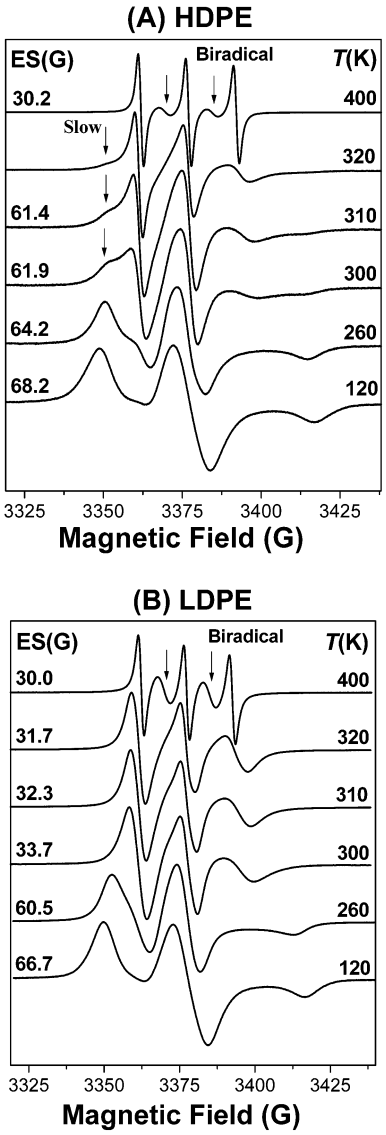

Figure 5. ESR spectra of the spin probe at the indicated temperatures in HDPE (A) and LDPE (B). The extreme separation, ES(G), is given for some spectra. Downward arrows in the spectra measured at 400 K point to the signals from the biradical. The low field signal from the "slow" component is indicated in (A) for the spectra at 300, 310, and 320 K.

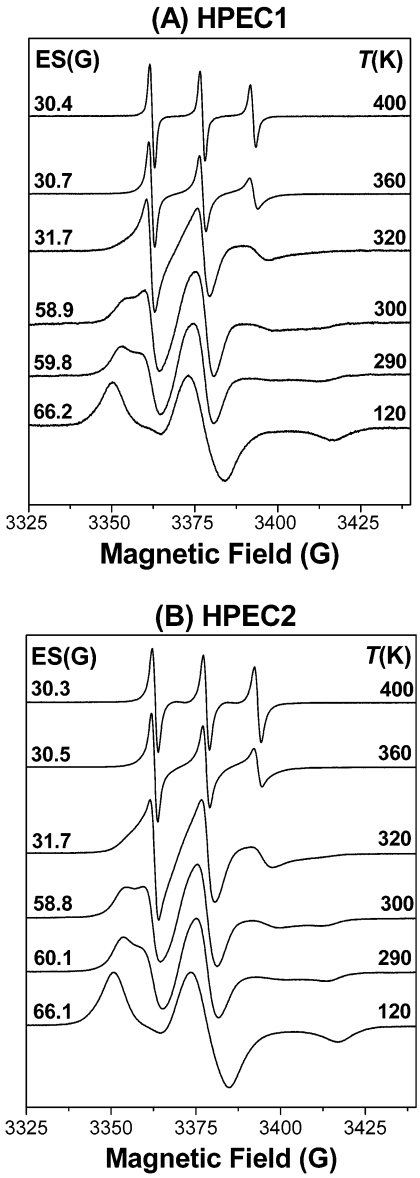

Figure 6. ESR spectra of the spin probe at the indicated temperatures in HPEC1 (A) and HPEC2 (B). The extreme separation, ES(G), is given on the left. At 300 K, % F = 36 in (A) and 29 in (B).

different thermal treatment during sample preparation: in the plaques prepared by injection molding the % F is higher. This was also the case for ABS.[16a]

Surprisingly, the extreme separation (ES) is slightly but consistently higher for HPEC1 compared to HPEC2 in the temperature range 240−280 K: At 240 K, ES is 64.3 and 63.7 G for HPEC1 and HPEC2, respectively; at 280 K, the values are 62.0 and 61.1 G. While this result suggests that HPEC1 is a more rigid matrix (although the amount of EPR is higher than in HPEC2), the spectra at 400 K suggest the opposite: the line widths of the three signals are lower in HPEC1. We note that the narrower lines in HPEC1 compared to HPEC2 are detected at 400 K, above the melting point of PE.

These results were clarified by two sets of experiments: First, the melting transitions in iPP, HPEC1, and HPEC2 were measured by DSC; the results are shown in Figure 7. Both HPEC samples show the crystallinity of PP, but the melting endotherm for PE is seen clearly only for HPEC1. The slightly larger ES in HPEC1 can therefore be assigned to the presence of the crystalline PE fraction.

Additional support for the higher content of crystalline PE in HPEC1 is reflected in the FTIR spectra of iPP, HPEC1, and HPEC2 (Figure 8). The peak at 730 cm^{-1} reflects the CH_2 rocking vibration in the crystalline phase and is an indicator of closely packed (crystalline) methylene chains; the peak at 720 cm^{-1} is associated with both amorphous and crystalline phases. The corresponding polarization is along the *a*-axis (730 cm^{-1} peak) and *b*-axis (720 cm^{-1} peak) of PE. The relative intensity of the two peaks can be used to estimate the relative crystallinity of PE samples.[28−32] The deconvolution of the signal from the CH_2 rocking vibration, based on Lorentzian line shapes, is shown for HPEC1 in Figure 8B and for HPEC2 in Figure 8C. The corresponding absorbance ratios A_{730}/A_{720} are 0.59 (HPEC1) and 0.44 (HPEC2), indicating a higher crystallinity in HPEC1, in agreement with DSC results (Figure 7). The IR spectra in Figure 8 also show a similar stereoregularity in PP, HPEC1, and HPEC2: the intensity ratio

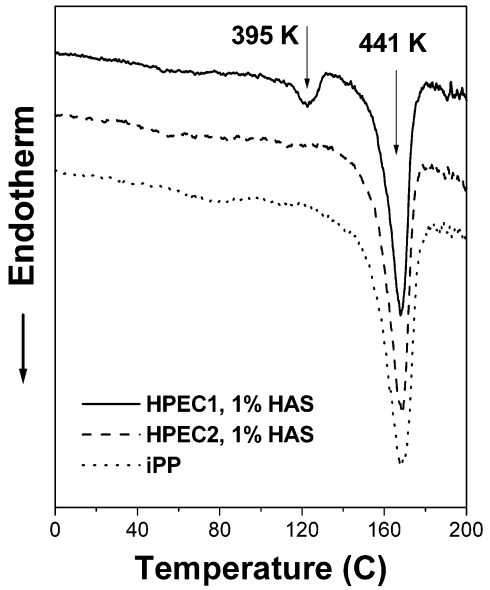

Figure 7. Thermal transitions of iPP, HPEC1, and HPEC2 measured by DSC.

of the absorptions at 998 and 973 cm^{-1} [9,33] is 0.80 ± 0.01 in the three systems.

Discussion

In this section we will discuss the nature of amorphous domains in semicrystalline polymers and the analogy between the results obtained in this study and the self-assembled polymeric systems such as ion-containing polymers and block copolymer micelles in aqueous media.

F and S Amorphous Domains in HPEC1 and HPEC2. The endothermic heats determined by DSC for the crystallinity peaks in iPP, HPEC1, and HPEC2 (Figure 7) cannot be translated into corresponding degrees of crystallinity because of the broad range of enthalpies of fusion, H_f, for iPP and PE available in the literature.[27] The degree of crystallinity of iPP, 58%, was calculated from the corresponding density. The crystallinity is strongly correlated with the regularity ratio, A_{998}/A_{973}.[34] On the basis of the same A_{998}/A_{973} ratio for iPP, HPEC1, and HPEC2 (Figure 8), we make the assumption that the corresponding degree of crystallinity of the PP component in the HPEC samples is similar to that of iPP: 58%. In support of this assumption, we also note that the DSC peak corresponding to PP has the same shape and appears at the same temperature in the three polymers, 441 ± 0.5 K. In the following step we used the endothermic heats determined by DSC, 74.0 J/g for iPP, 50.5 J/g for HPEC2, and 43.1 J/g for HPEC1, to calculate the wt % of crystalline PP in the HPEC samples. The percent of amorphous PP and EPR in the HPEC samples can also be deduced, as shown in Table 3. If we make the additional assumption that the probes have no preferred location in the various amorphous domains, we can now estimate how the various amorphous phases are represented in the F and S components present in the ESR spectra.

The amorphous phase content in the HPEC samples is the sum of amorphous PP and EPR contents; in the case of HPEC1 the sum must be reduced by the approximately 2−3% crystalline PE, deduced from the endothermic heat of 4.6 J/g measured by DSC (Figure 7) and H_f = 280 J/g for polyethylene. Therefore, we obtain that the amorphous phase content is 60% in HPEC2 and 63% in HPEC1. If we make the reasonable assumption that amorphous PP is represented by a slow component,[35] and consider that experimentally we determined % F = 41 in HPEC1 and 35 in HPEC2, we deduce that the fast component represents 21 wt % in HPEC2 and 26 wt % in HPEC1. The F component is ≈68% of the total EPR content in HPEC2 and ≈63% in HPEC1. In other words, about one-third of the EPR component is represented by a *slow* component: ≈$^1/_3$ of the elastomer phase is restrained by the crystalline domains. These deductions must be considered only semiquantitative, in view of the assumptions presented above.

Table 3. F and S Components in IPP, HPEC1, and HPEC2[a]

polymer	Δ*H*, J/g	cPP,[b] wt %	AmPP, wt %	EPR, wt %	amorphous phase, wt %	wt % EPR as F[d]
IPP	74.0	58	42	0	42	0
HPEC2	50.5	40	29	31	60	21
HPEC1[c]	43.1	34	25	41	63[b]	26

[a] Determined from DSC data. [b] cPP is crystalline PP; AmPP is amorphous PP; EPR is ethylene−propylene rubber; F is the fast component in the ESR spectra. [c] The sample contains 2−3 wt % crystalline PE. [d] Determined to fit the % F in the ESR spectra measured at 300 K.

Amorphous Domains in Semicrystalline Polymers. Polymers based on P and E units were among the first to be studied by the spin probe method, with 2,2,6,6-tetramethyl-4-hydroxypiperidin-1-oxyl benzoate (BzONO),[20,21,23] 2,2,6,6-tetramethyl-4-hydroxypiperidin-1-oxyl (HONO),[20] and 2,2,5,5-tetramethyl-3-oxazolidinyloxy (TMOZ)[22] as the reporters. The ESR spectra of the probes in iPP, amorphous PP, HDPE, and LDPE have been measured, some as a function of temperature. The main emphasis of these studies was the determination of T_{50G}, the temperature at which the extreme separation in the spectra of the probes is 50 G, and examination of the correlation with the glass transition temperature, T_g, measured by DSC and other methods. Some aspects of these early studies are relevant for the present study. The ESR spectra of BzONO in iPP consisted of two components, while only one component was reported in amorphous PP and in two other polymers, poly(butene-1) and poly(4-methylpentene-1), which are isotactic but amorphous.[23] The two spectral components in iPP were assigned to probes located in different amorphous phases consisting of isotactic (but not crystalline) and atactic PP. Implied in these results was the idea that crystalline domains have an effect on the spectra of the probe sites.

It is also interesting to compare the results for BzONO:[21] A small amount of the fast component was reported for both HDPE and iPP. Some of these results are similar, and some are different, compared to our data. In HDPE we also detected two spectral components; in iPP, however, only one component appears in our spectra, with broad lines even at high temperatures. We propose that the different results are due to the different spin probes used as reporters and also to possible variations in the degree of crystallinity of some polymers. A detailed study on samples with known degrees of crystallinity and using spin probes of different size is necessary in order to attempt a direct comparison.

The three-phase model for semicrystalline polymers, which considers the existence of an interphase charac-

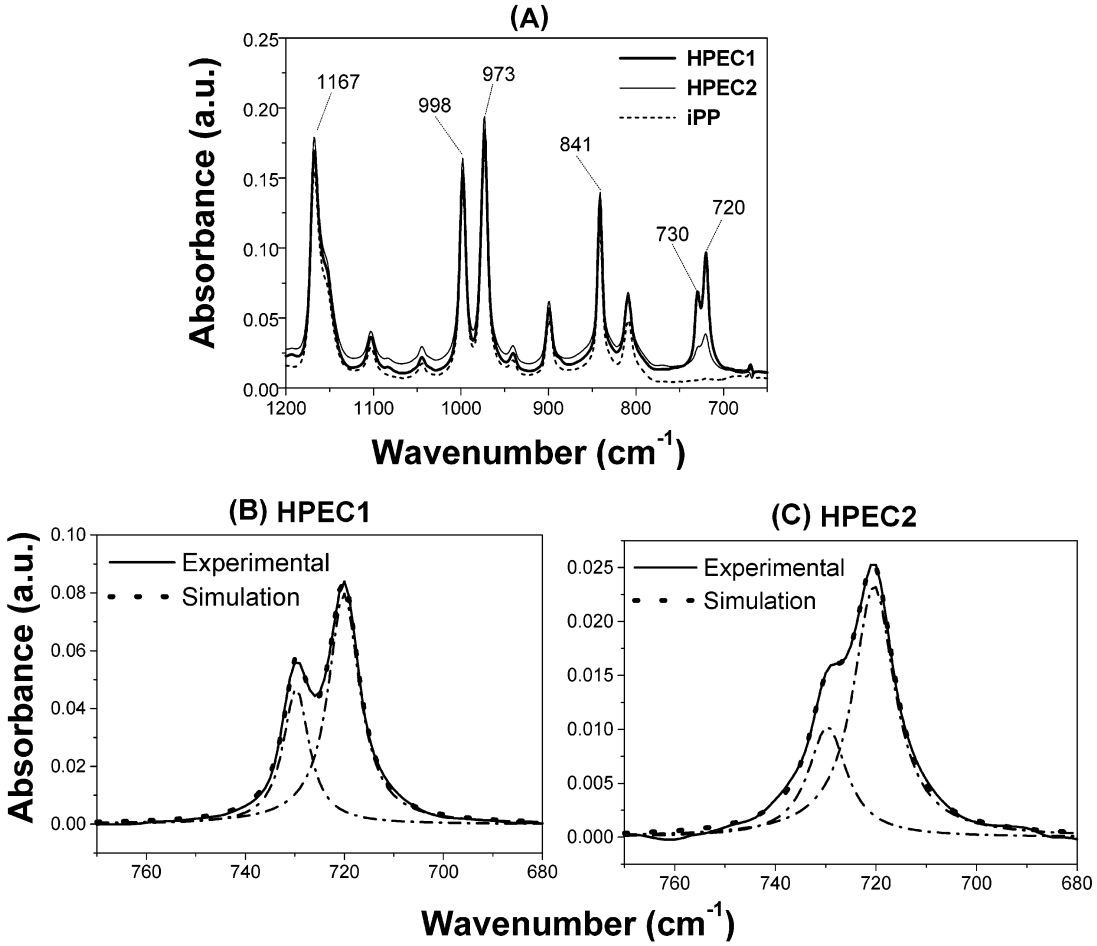

Figure 8. (A) FTIR spectra of iPP, HPEC1, and HPEC2. Peaks at 1167, 998, 973, and 841 cm^{-1} are the stereoregularity peaks for iPP. The deconvolution of the PE peaks at 720 and 730 cm^{-1} is shown for HPEC1 in (B) and for HPEC2 in (C).

terized by partial order, has received considerable support in the past 10 years from a variety of experimental and theoretical studies. The experimental studies have explored the mechanical properties of the interphase, differences in specific heat, small-angle X-ray scattering (SAXS), NMR, FTIR, and Raman spectra.[36−40] The picture that emerged from these studies is that the boundary between crystalline and totally disordered domains is not sharp. In some systems a broadening of the glass transition and an increase in T_g with increasing degree of crystallinity were observed. A decrease of the change in specific heat, C_p, beyond that expected for the amount of polymer that has crystallized, has also been detected in some cases and has been taken as an indicator of some rigidity in the amorphous phase. These phenomena have been rationalized by assuming the presence of a *rigid amorphous phase*.[36,37] This phase is considered the part of the amorphous phase that is modified by the proximity to the crystalline phase.

The results obtained in the present study are compatible with the concept of a rigid amorphous phase. The restraining effect of the crystalline domains is seen from the broad lines and the variation of the extreme separation in the ESR spectra of the nitroxide radicals and from the ratio of the F and S components. In addition to the existence of the interphase, the picture that emerged from the present study includes a *gradient* in dynamics of the interphase, which can be visualized directly from the spectra or by spectral simulations. In the case of iPP the dynamic range of amorphous phases is reflected in the unusually broad lines and the large values of the line widths used to simulate the experimental spectra. In the case of HDPE, the dynamic range is reflected in the detection of F and S components; additional details were delineated by comparison of HDPE and LDPE, which differ in the degree of crystallinity.

The amorphous phase is expected to be more restricted in the region between two crystalline domains, as shown in Figure 9. In other words, we expect that the restricted amorphous phase exist not only due to the gradual loss of order from polymeric crystals to the disordered phase, as suggested in the original paper of Flory,[41] but also because of restrictions arising from more than one proximal crystalline domain. This idea is supported by the results in HPEC1, where the presence of even a small amount of crystalline PE (2−3 wt % of the entire sample, corresponding to ≈10 wt % of the total E amount) leads to a larger ES in the ESR spectra of HAS−NO. The schematic representation of the restricted phase in Figure 9 also implies that higher crystallinity will lead to a larger part of the amorphous phase to become restricted and to a more dynamically restricted amorphous phase.

The advantage of the approach described here is that the nitroxide radicals are capable of detecting small differences in the dynamic behavior of the amorphous phases and of assessing the effect of the crystalline domains on the local dynamics at the probe site. The ESR spectra of the probes is also sensitive to the methods used to prepare the samples: slightly different

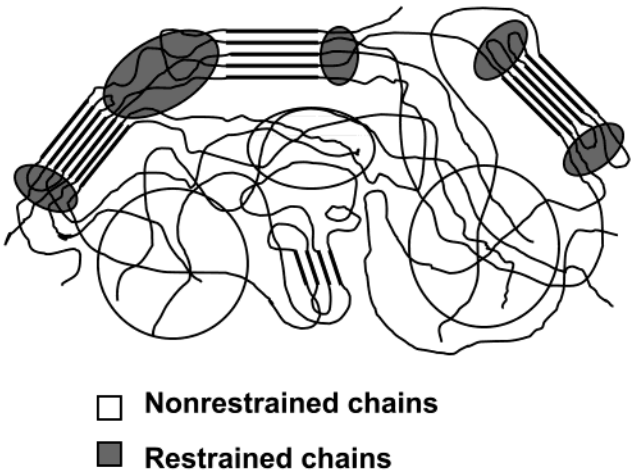

Figure 9. Schematic representation of the amorphous polymer chains restrained due to their proximity to the crystalline domains (dark gray areas) and not restrained (light gray areas). See text.

line widths and F/S ratios were determined in plaques prepared by injection molding and in samples prepared by melting of the polymer together with spin probe. In the case of HPEC, the deconvolution of the ESR spectra, together with DSC and FTIR data, led to the conclusion that $^1/_3$ of the elastomer phase is restrained by the crystalline domains.

The local details that are obtained with paramagnetic probes are not easy to obtain with scattering or microscopic methods of study, for instance SAXS and SEM.

Analogy with Self-Assembled Polymeric Systems. The concept of a dynamically restrained amorphous phase in semicrystalline polymers has important analogies in self-assembled polymeric systems, where the presence of an interphase has been demonstrated by spectroscopic methods. Two examples from our work will be presented.

Ion-Containing Polymers. The effect of ions on the polymer properties was described in a model that assumed clustering of the ions into ionic domains.[42] The model also predicted that the presence of the ionic domains has a restraining effect on the chains located in the immediate vicinity of the ion clusters.

The restraining effect of the ions on the chain mobility was detected experimentally in our studies by the use of a series of amphiphilic spin probes doped in aqueous micellar solutions of poly(ethylene-*co*-methacrylic acid) ionomers.[43,44] ESR spectra indicated that a clear micelle−solvent interface exists even at 360 K; inside the aggregate, however, the local mobility is high on the time scale of the ESR experiment, with typical correlation times of the probes $\approx 10^{-10}$ s/rad. Restricted mobility was detected in a layer of thickness of ≈10 Å from the aggregate−solvent interface and was attributed to constraints arising from the presence of proximal ionic groups. The major result from this study was the detection of gradual variations in the mobility of the probes, which reflected a *gradient* of dynamics in the aggregates: from restricted mobility near the ionomer−solvent interface to a much higher mobility toward the less polar regions of the aggregates, in both ionomer solutions and swollen membranes.

Block Copolymer Micelles. A second example from our work is the case of block copolymer micelles formed by poly(styrene-*co*-acrylic acid) (P(S-*co*-AA)) in an aqueous medium.[45] The ESR spectrum of the spin probe 5-doxyldecane (5DD) as a function of temperature in the range 120−360 K revealed three spectral components: One component was identified with the spin probe located in the polystyrene core of the micelle. A second component with extremely narrow lines appeared at ≈330 K and was assigned to the spin probe in the acrylic acid corona. The most relevant result for the present study was the appearance of a *third* spectral component at and above 350 K, which consisted of three lines that were much broader than the signals assigned to the probe in PAA; the ^{14}N hyperfine splitting, a_N, was however the same as in PAA. This third component was assigned to the inner parts of the PAA corona, close to PS chains.

Support for the restrictive effect of the core on the mobility of the corona can also be found in NMR[46,47] and fluorescence studies[48] of block copolymer micelles. These effects were observed in aqueous media for micelles that consisted of a core below its glass transition, typically polystyrene, and a hydrophilic corona, typically poly(acrylic acid) or poly(methacrylic acid).

In the ion-containing polymers and in the block copolymer micelles the interpretation was straightforward because the presence of both restricting and restricted domains was represented in the ESR spectra of the spin probes. In the case of HPEC and related systems, the crystalline domains are "blind spots" in the sense that their presence is not revealed directly in the ESR spectra of the probes, so their effect is more subtle, but not less clear: they create a gradient of dynamics in the amorphous phases that is detected by the spin probes with exceptional sensitivity.

Additional Comment. In a recent paper, the transport of oxygen in poly(ethylene naphthalate) (PEN) as a function of crystallization conditions was rationalized by assuming dedensification of the amorphous regions subjected to constraints by neighboring crystallites.[49] The density of the amorphous phase as a whole was expressed as a sum of two contributions: from the amorphous matrix and from the restricted amorphous phase. The picture reflected by the ESR spectra of the nitroxide radicals in HPEC and related polymers, described above, is slightly more complicated and consists of a *range* of amorphous phases differing in their dynamical properties.

Conclusions

The ESR spectra provided unambiguous evidence for location of the nitroxide radicals in a range of amorphous sites differing in their dynamical properties. The distribution of sites was explained by assuming that the crystalline domains exert a restraining effect on chains located in amorphous domains; in PE the restraining effect was more pronounced in the polymer with the higher crystallinity (HDPE) compared to LDPE. Additional support for this assumption was provided by FTIR spectra of HPEC and related polymers and by DSC.

The dynamically restrained phase evidenced by the spin probes is analogous to the "rigid amorphous phase" described in the literature. From ESR, DSC, and FTIR results we estimated that the restricted amorphous phase is $\approx^1/_3$ of the total amount of the elastomer (EPR) component in the HPEC samples. This study has demonstrated that nitroxide radicals are exceptionally sensitive to polymer morphology and can be used to extract parameters that describe the three-phase model for semicrystalline polymers.

The restraining effect of the crystalline domains on the dynamics in the amorphous phases is also analogous with phenomena detected in other systems; examples include the reduced mobility of polymer chains in the vicinity of ionic domains in ion-containing polymers and the motionally restrained corona layers close to the micellar core in block copolymer micelles in aqueous media.

Acknowledgment. This study was supported by the Polymers Program of the National Science Foundation. We thank Dow and Ciba Companies for the gift of the HPEC samples and HAS, respectively, and G. F. Pedulli (University of Bologna) and I. Dragutan (Bucharest) for the spin probe prepared by oxidation of Tinuvin 770. Special thanks are due to John L. Gerlock for his suggestions and help with sample preparation, to Mikhail M. Motyakin for sample preparation and initial ESRI measurements, and to Robert J. Meier (DSM, The Netherlands) for sharing with us his insight into the three-phase model of semicrystalline polymers.

References and Notes

(1) (a) Pukansky, B. In *Polymeric Materials Encyclopedia*; Salamone, J. C., Ed.; CRC Press: Boca Raton, FL, 1996; pp 6615−6623. (b) Tullo, A. H. *Chem. Eng. News* **2001**, *79*, 10−14.
(2) ESR spectroscopy is also known as EPR (electron paramagnetic resonance). In this paper we use ESR for the spectroscopy and EPR for the ethylene−propylene rubber.
(3) Albizzati, E.; Giannini, U.; Collina, G.; Noristi, L.; Resconi, L. In *Polypropylene Handbook*; Moore, E. P., Jr., Ed.; Hanser Publishers: Munich, 1996; Chapter 2, p 92.
(4) Mirabella, F. M. *Polymer* **1993**, *34*, 1729. (b) Mirabella, F. M. *J. Polym. Sci., Part B: Polym. Phys.* **1994**, *32*, 1205.
(5) Mirabella, F. M., Jr.; McFaddin, D. C. *Polymer* **1996**, *37*, 931.
(6) Xu, J.; Feng, L.; Yang, S.; Wu, Y.; Yang, Y.; Kong, X. *Polymer* **1997**, *38*, 4381.
(7) Feng, Y.; Hay, J. N. *Polymer* **1998**, *39*, 6723.
(8) Randall, J. C. *Polym. Prepr. (Am. Chem. Soc., Div. Polym. Chem.)* **1998**, *39* (1), 200.
(9) Zhu, X.; Yan, D.; Fang, Y. *J. Phys. Chem. B* **2001**, *105*, 12461.
(10) Kamfjord, T.; Stori, A. *Polymer* **2001**, *42*, 2767.
(11) Fan, Z. Q.; Zhang, Y.-Q.; Xu, J.-T.; Wang, H.-Tao.; Feng, L.-X. *Polymer* **2001**, *42*, 5559.
(12) Morris, H. R.; Monroe, B.; Ryntz, R. A.; Treado, P. J. *Langmuir* **1998**, *14*, 2426 and references therein.
(13) Pennington, B. D.; Ryntz, R. A.; Urban, M. W. *Polymer* **1999**, *40*, 4795.
(14) Fitchmun, D. R.; Mencik, Z. *J. Polym. Sci., Polym. Phys. Ed.* **1973,** *11*, 951.
(15) Motyakin, M. V.; Gerlock, J. L.; Schlick, S. *Macromolecules* **1999**, *32*, 5463. (b) Kruczala, K.; Motyakin, M. V.; Schlick, S. *J. Phys. Chem. B* **2000**, *104*, 3387. (c) Motyakin, M. V.; Schlick, S. *Macromolecules* **2001**, *34*, 2854. (d) Motyakin, M. V.; Schlick, S. *Polym. Degrad. Stab.* **2002**, *76*, 25. (e) Motyakin, M. V.; Schlick, S. *Macromolecules* **2002**, *35*, 3984.
(16) Varghese, B.; Schlick, S. *J. Polym. Sci., Part B: Polym. Phys.* **2002,** *40*, 415. (b) Varghese, B.; Schlick, S. *J. Polym. Sci., Part B: Polym. Phys.* **2002,** *40*, 424.
(17) Bokria, J. G.; Schlick, S. *Polymer* **2002** *43*, 3239.
(18) Kruczala, K.; Bokria, J. G.; Schlick, S. *Macromolecules* **2003**, *36*, 1909.
(19) Brigati, G. University of Bologna, personal communication.
(20) Rabold, G. P. *J. Polym. Sci., Part A1* **1969**, *7*, 1203.
(21) Kumler, P. L.; Boyer, R. F. *Macromolecules* **1976**, *9*, 903.
(22) Cameron, G. G. In *Molecular Motion in Polymers by ESR*; Boyer, R. F., Keinath, S. E., Eds.; Harwood Academic Publishers: New York, 1980; p 55.
(23) Kumler, P. L. In *Molecular Motion in Polymers by ESR*; Boyer, R. F., Keinath, S. E., Eds.; Harwood Academic Publishers: New York, 1980; p 189.
(24) Schneider, D. J.; Freed, J. H. In *Biological Magnetic Resonance*; Berliner, L. J., Reuben, J., Eds.; Plenum: New York, 1989; Vol. 8, p 1. (b) Budil, D. E.; Lee, S.; Saxena, S.; Freed, J. H. *J. Magn. Reson. A* **1996**, *120*, 155.
(25) Rabello, M. S.; White, R. J. *Polymer* **1997**, *38*, 6379, 6389.
(26) Gensler, R.; Plummer, C. J. G.; Kausch, H.-H.; Kramer, E.; Pauquet, J.-R.; Zweifel, H. *Polym. Degrad. Stab.* **2000**, *67*, 195.
(27) *Polymer Handbook*, 4th ed.; Brandrup, J., Immergut, E. H., Grulke, E. A., Eds.; John Wiley & Sons: New York, 1999; pp V/9−19 (PE); V/21−30 (PP).
(28) Tobin, M. C.; Carrano, M. J. *J. Polym. Sci.* **1957**, *24*, 93.
(29) Snyder, R. G.; Maroncelli, M.; Strauss, H. L.; Hallmark, V. M. *J. Phys. Chem.* **1986**, *90*, 5623.
(30) Lin-Vien, D.; Colthup, N. B.; Fateley, W. G.; Grasselli, J. G. *The Handbook of Infrared and Raman Characteristic Frequencies of Organic Molecules;* Academic Press: Boston, 1991; p 15.
(31) Koenig, J. L. *Spectroscopy of Polymers;* American Chemical Society: Washington, DC, 1992; Chapter 4.
(32) Smith, B. *Infrared Spectral Interpretation;* CRC Press: Boca Raton, FL, 1999; pp 38, 180.
(33) Carlson, E. D.; Krejchi, M. T.; Shah, C. D.; Terakawa, T.; Waymouth, R. M.; Fuller, G. G. *Macromolecules* **1998**, *31*, 5343.
(34) Philips, R. A.; Wolkowicz, M. D. L. In *Polypropylene Handbook*; Moore, E. P., Jr., Ed.; Hanser Publishers: Munich, 1996; Chapter 3, pp 113−176.
(35) Franchi, P.; Lucarini, M.; Pedulli, G. F.; Bonora, M.; Vitali, M. *Macromol. Chem. Phys.* **2001**, *202*, 1246 and references therein.
(36) Cheng, S. Z. D.; Wunderlich, B. *Macromolecules* **1988**, *21*, 789.
(37) Wunderlich, B. *Thermal Analysis;* Academic Press: Boston, 1990. (b) *Prog. Polym. Sci.* **2003**, *28*, 383.
(38) Mandelkern, L. *Acc. Chem. Res.* **1990**, *23*, 380.
(39) Naylor, C. C.; Meier, R. J.; Kip, B. J.; Williams, K. P. J.; Mason, S. M.; Conroy, N.; Gerrrard, D. L. *Macromolecules* **1995**, *28*, 2969 and references therein.
(40) Chen, H.-L.; Li, H.-C.; Huang, Y.-Y.; Chiu, F.-C. *Macromolecules* **2002**, *35*, 2417.
(41) Flory, P. J. *J. Phys. Chem.* **1949**, *17*, 233.
(42) Eisenberg, A.; Hird, B.; Moore, R. B. *Macromolecules* **1990**, *23*, 4098.
(43) Kutsumizu, S.; Schlick, S. *Macromolecules* **1997**, *30*, 2329.
(44) Kutsumizu, S.; Goto, M.; Yano, S.; Schlick, S. *Macromolecules* **2002**, *35*, 6298.
(45) Unpublished results from this laboratory. The block copolymers micellar solutions were prepared by A. Meyer and A. Eisenberg (McGill University, Montreal, Canada).
(46) Kriz, J.; Masar, B.; Doskocilova, D. *Macromolecules* **1997**, *30*, 4391.
(47) Kriz, J.; Kurkova, D.; Kadlec, P.; Tuzar, Z.; Plestil, J. *Macromolecules* **2000**, *33*, 1978.
(48) Stepanek, M.; Prochaska, K.; Brown, W. *Langmuir* **2000**, *16*, 2502.
(49) Hu, Y. S.; Liu, R. Y. F.; Zhang, L. Q.; Rogunova, M.; Schiraldi, D. A.; Nazarenko, S.; Hiltner, A.; Baer, E. *Macromolecules* **2002**, *35*, 7326.

MA025700Y